Development 130, 2213-2224

doi:10.1242/dev.00445

Fgf3 and Fgf8 dependent and independent transcription factors are required for otic placode specification

Dong Liu[1], Hsin Chu*, Lisa Maves[1], Yi-Lin Yan[1], Paul A. Morcos[2], John H. Postlethwait[1] and Monte Westerfield[1,†]

[1]Institute of Neuroscience, University of Oregon, Eugene, OR 97403, USA
[2]Gene Tools, LLC, 1 Summerton Way, Philomath, OR 97370, USA
*Deceased
[†]Author for correspondence (e-mail: monte@uoneuro.uoregon.edu)

Accepted 19 February 2003

SUMMARY

The vertebrate inner ear develops from the otic placode, an ectodermal thickening that forms adjacent to the presumptive hindbrain. Previous studies have suggested that competent ectodermal cells respond to signals from adjacent tissues to form the placode. Members of the Fgf family of growth factors and the Dlx family of transcription factors have been implicated in this signal-response pathway. We show that compromising Fgf3 and Fgf8 signaling blocks ear development; only a few scattered otic cells form. Removal of *dlx3b*, *dlx4b* and *sox9a* genes together also blocks ear development, although a few residual cells form an otic epithelium. These cells fail to form if *sox9b* function is also blocked. Combined loss of Fgf signaling and the three transcription factor genes, *dlx3b*, *dlx4b* and *sox9a*, also completely eliminates all indications of otic cells. Expression of *sox9a* but not *dlx3b*, *dlx4b* or *sox9b* requires Fgf3 and Fgf8. Our results provide evidence for Fgf3- and Fgf8-dependent and -independent genetic pathways for otic specification and support the notion that Fgf3 and Fgf8 function to induce both the otic placode and the epithelial organization of the otic vesicle.

Key words: *dlx3b*, *dlx4b*, Inner ear, Morpholino, Olfactory placode, *sox9a*, *sox9b*, Zebrafish

INTRODUCTION

In vertebrates, the initial morphological event in inner ear development is the formation of the embryonic otic placode, a thickening of the head ectoderm adjacent to the developing hindbrain. Through interactions with adjacent tissues and incorporation of additional cells from the neural crest and mesoderm, the placode develops into the otic vesicle, also called the otocyst, an epithelial structure with sharply defined borders (Fritzsch et al., 1997; Noden and van de Water, 1986; Couly et al., 1993). Later, the otic vesicle forms the inner ear including its neurons and most of its structural elements. A variety of studies suggest that cells are specified to form the otic placode in response to inductive signals from neighboring tissues (Fritzsch et al., 1997; Torres and Giráldez, 1998; Baker and Bronner-Fraser, 2001; Whitfield et al., 2002) including the underlying mesendoderm (Jacobson, 1963; Mendonsa and Riley, 1999) and the adjacent hindbrain (Stone, 1931; Harrison, 1945; Waddington, 1937; Woo and Fraser, 1998; Hutson et al., 1999).

Although the precise molecular nature of the signals that induce cells to form the otic placode is still unknown, several studies implicate Fgf3 and Fgf8, members of the Fgf family of signaling peptides. In zebrafish, the genes that encode these peptides are expressed in the presumptive hindbrain by late gastrula stages and *fgf3* is also expressed at this stage in the underlying mesendoderm (Phillips et al., 2001). Fgf3 and Fgf8 mediate inter-rhombomere signaling required for hindbrain patterning (Maves et al., 2002). Loss of Fgf3 function in chick (Represa et al., 1991) or of both Fgf3 and Fgf8 functions together in zebrafish (Phillips et al., 2001; Léger and Brand, 2002; Maroon et al., 2002) is sufficient for near or total ablation of otic tissue, and ectopic expression of Fgf3 (Vendrell et al., 2000) or Fgf2 (Lombardo and Slack, 1998) results in the formation of ectopic otic vesicles in frog and chick.

To understand how Fgf signals may specify cells to form the otic placode, we studied the functions of four transcriptions factors expressed by otic placode precursor cells in zebrafish, *dlx3b* (previously called *dlx3*) (Ekker et al., 1994), *dlx4b* (previously called *dlx7*) (Stock et al., 1996; Ellies et al., 1997), *sox9a* (Chiang et al., 2001; Yan et al., 2002) and *sox9b* (Chiang et al., 2001; Li et al., 2002). The *dlx3b* and *dlx4b* genes are closely linked, as are their mammalian orthologues (Nakamura et al., 1996; Morasso et al., 1997), probably because of ancestral tandem duplication in the lineage giving rise to vertebrates (Stock et al., 1996). We have previously shown that early precursor cells of the otic placode express *dlx3b* before any overt morphological signs of differentiation (Ekker et al., 1992; Akimenko et al., 1994); *dlx4b* has a similar expression pattern (Ellies et al., 1997). By prim-5 stage (24 hours), only a subset of cells in the otic vesicle still expresses *dlx3b* (Ekker et al., 1992).

In humans, a small deletion in the *DLX3* gene is thought to be responsible for Trichodentoosseous syndrome (TDO) (Price et al., 1998). Individuals with TDO exhibit a variety of clinical problems, including ear, tooth and skull defects (Shapiro et al., 1983), consistent with the expression pattern of *Dlx3* in mice (Robinson and Mahon, 1994) and zebrafish (Akimenko et al., 1994). A knockout mutation of *Dlx3* in mice results in embryonic lethality due to placental insufficiency before the ear forms (Morasso et al., 1999). Analysis of *dlx3b* and *dlx4b* in zebrafish suggested that they may serve redundant roles in otic development (Solomon and Fritz, 2002).

We have previously shown that the zebrafish *sox9a* and *sox9b* genes are duplicate orthologues of the human *SOX9* gene and that both genes are expressed in the otic placode (Chiang et al., 2001). In humans, *SOX9* haploinsufficiency results in campomelic dysplasia, characterized by abnormal development of the long bones and associated sex reversal (Foster et al., 1994; Wagner et al., 1994; Hageman et al., 1998; Cameron et al., 1996; Huang et al., 2001; Vidal et al., 2001). Most patients die of respiratory distress during the neonatal period, but one who survived through adolescence had hearing loss (Houston et al., 1983). Studies in mouse have shown that *Sox9* is expressed in the developing otic capsule (Kanzler et al., 1998). Heterozygous *Sox9* mutant mice show phenotypes similar to individuals with campomelic dysplasia and die at birth (Bi et al., 2001). Our analysis of zebrafish mutants demonstrated that *sox9a* is required for cartilage development (Yan et al., 2002).

To analyze the potential functions of *dlx3b*, *dlx4b* and *sox9a* in otic development, we characterized a deficiency mutation we previously isolated [*Df(LG12)dlx3b*^{b380}, called *Df*^{b380}] (Fritz et al., 1996) that lacks all three genes. We found that homozygous *Df*^{b380} mutants completely lack otic placodes and fail to form a differentiated otic vesicle or inner ear, although a few residual cells express genes characteristic of the developing inner ear. Knock down of all three genes by injection of morpholino antisense oligonucleotides (MOs) produces these phenotypes in wild-type embryos, and injection of wild-type mRNAs from all three genes together is sufficient for phenotypic rescue of the ear defects in homozygous *Df*^{b380} mutants. The residual cells fail to form if *sox9b* function is also blocked. We analyzed Fgf function using *fgf3*-MOs and *ace* (*fgf8*$^{-}$) mutants and found that *sox9a*, but not *dlx3b* or *dlx4b*, expression depends on Fgf signaling, and that the residual otic cells in homozygous *Df*^{b380} mutants fail to form if *fgf8* function is also absent. Our results demonstrate that Fgf3- and Fgf8-dependent (*sox9a*) and -independent (*dlx3b* and *dlx4b*) transcription factors are required for specification of the otic placode. Moreover, we found that the residual otic cells form a small epithelial ball characteristic of the early otic vesicle in *Df*^{b380} mutants but not in the absence of Fgf3 and Fgf8 signaling, thus indicating a role of Fgfs in induction of both the otic placode and the epithelial organization of the otic vesicle.

MATERIALS AND METHODS

Animals

Embryos and adults were obtained from the University of Oregon zebrafish facility. Animals were maintained and embryos produced using standard procedures (Westerfield, 2000). Embryos were staged according to standard criteria (Kimmel et al., 1995) or by hours post fertilization at 28°C (h).

The wild-type line used was AB (University of Oregon, Eugene, OR). The *Df(LG12)dlx3b*^{b380} strain name has been approved by the zebrafish nomenclature committee (http://zfin.org/zf_info/nomen_comm.html) and we refer to homozygous mutants as *Df*^{b380}. The *acerebellar*^{ti282a} (*ace*) line, a strong hypomorphic allele of *fgf8*, has been described previously (Brand et al., 1996); we refer to the homozygous mutants as *fgf8*$^{-}$. Heterozygotes for both *Df*^{b380} and *fgf8*$^{-}$ genotypes were obtained by crossing *Df*^{b380} and *acerebellar*^{ti282a} carriers. Homozygous *Df*^{b380} mutants were primarily scored by their lack of somites; homozygous *ace* mutant embryos were scored by their loss of the cerebellum. Homozygous *Df*^{b380}*;fgf8*$^{-}$ embryos were scored with both criteria.

The *jellyfish* (*jef*) mutation (*jef*^{hil134}), which results from the insertion of a retrovirus (Amsterdam et al., 1999), disrupts *sox9a*. Exon 2 is skipped in the splicing in *jef*^{hil134} mutants, leading to a truncated protein that lacks the C-terminal half of the HMG domain (Yan et al., 2002). *jef*^{hil134} shows a more severe otic phenotype than *jef*^{tw37} (data not shown), which in theory should produce a truncated protein that lacks a large part of HMG and the entire C terminus.

Genes, markers and mapping

Approved gene and protein names that follow the zebrafish nomenclature conventions (http://zfin.org/zf_info/nomen.html) are used according to http://zfin.org. To map the deletion boundaries and the genes and markers missing from the deficient region, we used primers for genes and markers on LG12 to amplify expected bands from *Df*^{b380} genomic DNA by PCR.

In situ hybridization, mRNA synthesis and rescue

cDNA probes that detected the following genes were used: *dlx3b* (Ekker et al., 1992); *dlx4b* (Stock et al., 1996); *sox9a* (Chiang et al., 2001); *egr2* (*krox-20*) (Oxtoby and Jowett, 1993); *cldna* (Kollmar et al., 2001); *fn1* (Zhao et al., 2001) and *pax2a* (Krauss et al., 1991). Probe synthesis and single or double-color in situ hybridization (whole-mount) were performed essentially as previously described (Thisse et al., 1993; Jowett and Yan, 1996; Whitlock and Westerfield, 2000), except for minor modifications. We purified the in vitro synthesized mRNA and probes using an RNeasy mini column (Qiagen GmbH). Instead of NBT/BCIP (Boehringer), we used BM purple (Boehringer) to develop color at room temperature for more than 40 hours. We usually removed the yolks from young embryos using forceps. Embryos were mounted in phosphate-buffered saline (PBS) and photographed using a Zeiss Axiophot 2 microscope.

In vitro mRNA synthesis was performed using an RNA synthesis kit (Ambion). A partial *dlx3b* cDNA with a complete ORF (990 bp) was subcloned into pXT7 (Dominguez et al., 1995) at the *Eco*RI and *Spe*I sites. The plasmid was restricted with *Xba*I, and the linear DNA served as a template to generate *dlx3b* mRNA using T7 RNA polymerase. The complete *dlx4b* ORF was amplified by PCR and cloned into the pCRT7/CT-TOPO vector (Invitrogen). The resulting plasmid was linearized with *Pme*I and used as a template to synthesize *dlx4b* mRNA using T7 RNA polymerase. The recognition site of *dlx4b*-MO (see Morpholinos) on *dlx4b* mRNA was eliminated. This *dlx4b* mRNA could partially restore *dlx4b* activity if co-injected with *dlx4b*-MO, as judged by a restoration of *dlx4b*-MO-induced reduction of the median fin fold (data not shown). A full-length *sox9a* cDNA was cloned into pCDNA3 vector (Clontech). After linearizing with *Apa*I, the plasmid was used as a template to synthesize *sox9a* mRNA with T7 RNA polymerase.

For rescue experiments, we injected wild-type RNA into *Df*^{b380} embryos. We also injected a YAC clone that contains both the *dlx3b* and *dlx4b* genes (a gift from Angel Amores) and a shorter cosmid clone that contains the *dlx3b* gene with 0.8 kb of 3′ sequence. We obtained similar rescue as with *dlx3b* mRNA alone. The combination of the *dlx3b-dlx4b* YAC or cosmid DNA with a *sox9a* expression

vector (driven by a CMV promoter/enhancer) resulted in similar rescue as obtained with injection of all three wild-type mRNAs (*dlx3b*, *dlx4b* and *sox9a*). For both DNA and RNA injections, we delivered about 1 nl of solution into the cytoplasm of one-cell stage embryos. The concentrations of the injection solutions were 50-100 ng/μl (DNA) and 200-500 ng/μl (RNA). For injection of all three mRNAs, we used no more than 750 ng/μl total mRNA.

Morpholinos

Morpholino antisense oligonucleotides (MOs) were obtained from Gene Tools (Philomath, OR). Translation blocking MOs were: *dlx3b*-MO, 5′-ATGTCGGTCCACTCATCCTTAATAA-3′; *dlx4b*-MO, 5′-GCCCGATGATGGTCTGAGTGCTGC-3′; *sox9a*-MO, 5′-TCAGGTAGGGGTCGAGGAGATTCAT-3′; *fgf3*B, 5′-GGTCCCATCAAAGAAGTATCATTTG-3′; and *fgf3*C, 5′-TCTCGCTGGAATAGAAAGAGCTGGC-3′. Splice blockers were: *sox9bE1I1*, 5′-GTGTGTTTCTGACGAGTTTGCCGAG-3′; *sox9bI2E3*, 5′-GCCCTGAGACTGACCTGCACACACA-3′; and *fgf8*E2I2, 5′-TAGGATGCTCTTACCATGAACGTCG-3′; *fgf8*E3I3, 5′-CACATACCTTGCCAATCAGTTTCCC-3′. We described the *sox9a*-MOs that block pre-mRNA splicing previously (Yan et al., 2002). A combination of both *fgf8* splice-blocking MOs (*fgf8*-MO; 2.5 ng/each) was used to inject one- to two-cell stage embryos (Draper et al., 2001). We blocked pre-mRNA splicing by the injection of a combination of both *sox9b*-MO oligonucleotides (at 1 μg/μl each). As a control for the *sox9b*-MO, we visualized the nuclear localization of *sox9b* messenger by in situ hybridization (Y.Y. and D.L., unpublished). The concentration of single translation blocking MOs was 3μg/μl for *dlx3b*, *dlx4b* and *sox9a*. Combinatory MO injections were as follows: *dlx3b*+*dlx4b*-MOs, 3+1.5 μg/μl; *dlx3b*+*dlx4b*+*sox9a*-MOs, 3+1.5+1.5 μg/μl; and *sox9a*-MOs (splicing blockers) 5+5 μg/μl. To generate *fgf3-MO;fgf8*$^{-}$ embryos, *fgf3*B and *fgf3*C-MOs at 1 and 0.25 μg/μl, respectively, were used (Maves et al., 2002). About 1-3 nl of MO solution was injected into the cytoplasm of one-cell stage embryos. We have previously provided data to demonstrate the efficacy of the *fgf3*-MOs (Maves et al., 2002).

Dlx3b monoclonal antibody

We synthesized the complete *dlx3b* ORF using gene-specific primers and the Herculase enhanced polymerase blend (Strategene) and ensured that it is error-free by sequencing in both directions. We cloned the *dlx3b* ORF DNA fragment into the pCRT7/CT-TOPO vector (Invitrogen). By following the manufacturer's instructions, we introduced the resulting pCRT7dlx3b into host BL21(DE3)pLysE and grew the bacteria in the presence of appropriate antibiotics. SDS-PAGE electrophoresis analysis indicated strong expression of soluble Dlx3b fusion protein with the predicted molecular weight.

After one round of nickel-charged Sepharose purification (PreBond), 95% pure fusion protein was run on a native polyacrylamide gel. We eluted a small amount of the single protein band directly from the gel and used 0.2 mg of the purified fusion protein to raise monoclonal antibodies (University of Oregon Monoclonal Antibody Facility). Out of 10 positive clones identified by ELISA, we chose a clone (α-Dlx3b) that recognized wild-type embryos but not *Df*^{b380} mutants by whole-mount immunocytochemistry. The distribution of the antibody labeling is comparable with that of the mRNA in situ probe for *dlx3b*.

Immunocytochemistry

Embryos were fixed in 4% paraformaldehyde in PBS overnight at 4°C. After fixation, embryos were rinsed with PBS twice at room temperature for 20 minutes and then blocked in PBDTX (PBS with 1% bovine serum albumin, 1% DMSO, pH 7.3, and 0.1% Triton X-100) with 2% normal goat serum (NGS) for 30 minutes. Embryos were then incubated overnight at 4°C in primary antibodies at the following dilutions in PBDTX with 2% NGS: α-Pax2, 1:200 (BAbCO) and α-Dlx3b, 1:50. After PBDTX rinses to wash away the excess antibody, embryos were incubated in secondary antibody goat anti-rabbit or anti-mouse Alexa Fluor 488 (Molecular Probes) at 1:200 dilution in PBDTX with 2% NGS for 5 hours at room temperature or at 4°C overnight. Embryos were then rinsed in PBS and analyzed using a Zeiss Axiophot 2 microscope.

RESULTS

Cells of the presumptive otic placode express three transcription factor genes, *dlx3b*, *dlx4b* and *sox9a*

We have previously cloned the zebrafish *dlx3b* gene and showed that cells of the developing otic placode express *dlx3b* and *sox9a* (Ekker et al., 1992; Akimenko et al., 1994; Yan et al., 2002). Scattered cells on the ventral side of the embryo begin expressing *dlx3b* by mid-gastrula stages (Akimenko et al., 1994). As gastrulation proceeds, a band of strongly expressing cells coalesces at the lateral edge of the presumptive neural plate (Fig. 1A), while expression on the ventral side disappears. When the neural plate forms and cells move toward the dorsal midline in convergence, *dlx3b* expression is progressively restricted to two groups of cells in this band. These two groups of *dlx3b*-expressing cells probably correspond to the presumptive olfactory (Whitlock and Westerfield, 2000) and otic (Akimenko et al., 1994) placodes, even though there is no sign of morphological differentiation of the placodes until a few hours later. Shortly before the otic placode is visible morphologically, *dlx3b* expression is restricted to cells in the position where the placode will form and from then onwards, placode cells express *dlx3b* (Fig. 1B,C) (Akimenko et al., 1994).

The *dlx4b* gene, closely linked to *dlx3b* (Stock et al., 1996), has a similar although non-identical expression pattern (Fig. 1D-F). Expression of *dlx4b* first appears slightly later than *dlx3b* and, unlike *dlx3b*, on the dorsal side of the embryo. By the end of gastrulation, *dlx4b* expression is concentrated in a band of cells at the lateral edge of the neural plate and overlaps *dlx3b* expression throughout segmentation stages.

sox9a expression starts at about the same developmental stage as *dlx3b*. Unlike the two Dlx genes, *sox9a*-expressing cells are not observed around the lateral edge of the neural plate or in the olfactory placode. Instead, initial *sox9a* expression in the region of the hindbrain is limited to the presumptive otic placode, where it overlaps with *pax2a* expression (not shown). By segmentation stages, cells in the region of rhombomere 4 also express *sox9a*, although at somewhat lower levels than in the placode (Fig. 1G,H).

The *Df*^{b380} deficiency lacks the *dlx3b*, *dlx4b* and *sox9a* genes and blocks formation of the ear

To study the potential functions of Dlx genes in specification of the otic placode, we isolated a deficiency mutation, *Df(LG12)dlx3b*^{b380} (*Df*^{b380}) (Fritz et al., 1996), that removes the *dlx3b* locus. We identified the mutation in a screen for deficiencies based on multiplex PCR amplification of genomic DNA from haploid offspring of females carrying γ-ray induced mutations (Fritz et al., 1996). We initially identified the *Df*^{b380} mutation by the absence of a PCR amplification product from the *dlx3b* gene. We subsequently mapped the *dlx3b* gene to LG12 of the zebrafish genetic map and showed that the *Df*^{b380} mutation removed 21-24 cM of LG 12 that also contains

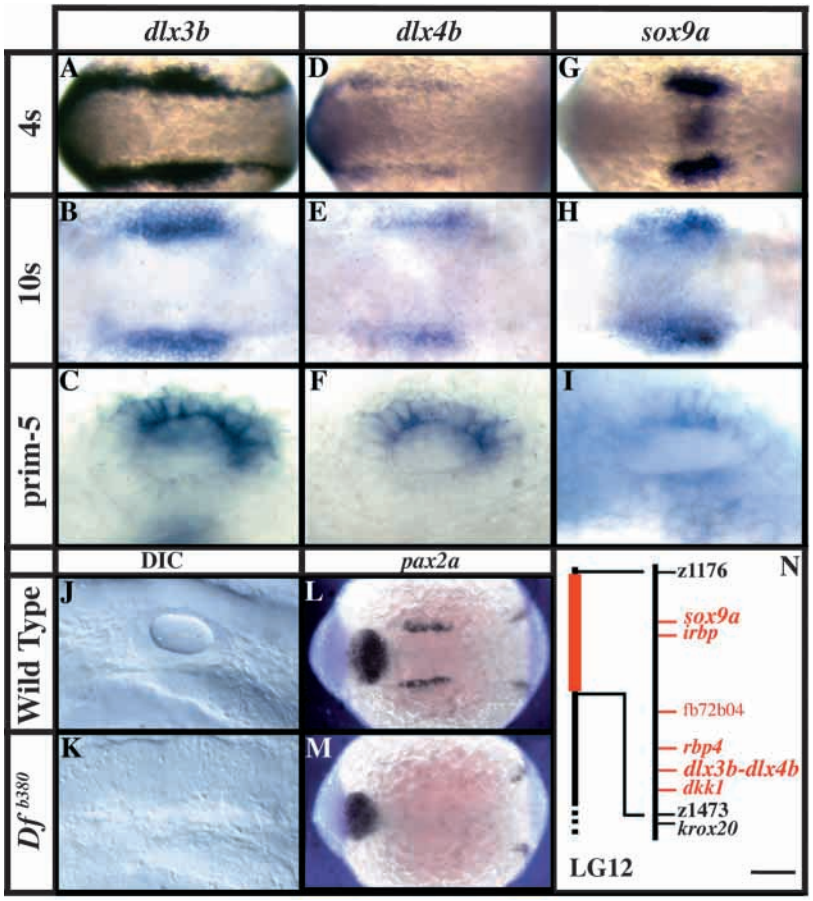

Fig. 1. Cells of the otic placode and vesicle express three transcription factor genes, *dlx3b*, *dlx4b* and *sox9a* required for inner ear development. (A,D,G) Cells of the presumptive otic placode express all three genes at the four-somite stage (4s); other cells along the lateral edge of the neural plate express *dlx3b* and *dlx4b*. (B,E,H) By the 10-somite stage (10s) cells throughout the placode express all three genes. (C,F,I) Later, by prim-5 stage (24 h), a subset of cells in the vesicle expresses *dlx3b* and *dlx4b*; other cells express *sox9a*. Throughout these stages, *dlx4b* expression is similar to but weaker than *dlx3b* expression. Other sites of expression are not shown. (J,L) Wild-type embryos exhibit an otic vesicle in live embryos (DIC, differential interference contrast optics) at prim-5 (24h) stage (J) and *pax2a* expression in the presumptive otic placode at the six-somite stage (L). (K,M) Neither the vesicle (K) nor early *pax2a* expression in the presumptive placode (M) is apparent in Df^{b380} mutants (38/38 Df^{b380} embryos). (N) The *dlx3b*, *dlx4b* and *sox9a* genes are closely linked on the same chromosome and are removed by the Df^{b380} deficiency mutation. (Left) Schematic map of LG12 showing the region of the Df^{b380} deficiency in red (not to scale). (Right) We localized *dlx3b*, *dlx4b* and *sox9a* to LG12 by mapping them relative to SSLP markers and other genes (as shown) using the LN54 radiation hybrid panel (Hukriede et al., 1999). We estimated the extent of the Df^{b380} deficiency based on our ability to amplify flanking SSLP markers, z1176 and z1473, by PCR using Df^{b380} homozygous mutant DNA. These two SSLP markers are separated by 21 cM on the HS and 24 cM on the MGH meiotic panels, and by 296 cR on the T51 radiation hybrid panel (http://zfin.org). Missing genes are shown in red. (A,B,D,E,G,H,L,M) Dorsal views, anterior towards the left; (C,F,I,J,K) side views, anterior towards the left, dorsal towards the top. Scale bar in N: 60 μm for A,D,G; 33 μm for B,E,H; 22 μm for C,F,I; 77 μm for J,K; 145 μm for L,M; 5 cM for N.

several other genes (Fig. 1N), including *dlx4b* (Stock et al., 1996) and *sox9a* (Chiang et al., 2001).

Homozygous Df^{b380} mutants fail to form an ear. We observed no otic placode or vesicle in live mutant embryos using Nomarski optics (Fig. 1K) and initial expression of *pax2a*, a marker of otic precursor cells in this region, is also absent (Fig. 1M). Other sites of *pax2a* expression (Püschel et al., 1992) appear normal in Df^{b380} mutants, including optic stalk, mid-hindbrain junction and pronephros, although *pax2a* expression is elevated in the branchial arches (data not shown). Homozygous Df^{b380} mutants also fail to form olfactory organs. Because olfactory organs form from ectodermal placodes that, like the otic placodes, express *dlx3b* and *dlx4b*, this associated phenotype may indicate a common pathway mediated by *dlx3b* and *dlx4b* for specification of these two sensory structures, as we (Akimenko et al., 1994) and others (Torres and Giraldez, 1998; Solomon and Fritz, 2002) have previously suggested. Heterozygous (Df^{b380}/+) individuals develop with no obvious abnormalities.

Despite this apparent lack of otic induction, a few residual cells express characteristics of otic cells in Df^{b380} mutants. By prim-5 stage (24 h), ~30% of Df^{b380} mutant embryos form a patch of 10-20 *pax2a*-expressing cells (Fig. 2B) lateral to hindbrain rhombomere 5 in the region where the otic vesicle normally develops in wild-type embryos. This *pax2a*-positive patch of cells is apparent in 80% of embryos (n=43) by prim-15 (30 h) and in all embryos (n=14) by the second day of development. Consistent with their differentiation as otic cells, these cells express other otic markers, including *fn1* (Fig. 2E) and *claudin a* (*cldna*), a marker of the otic epithelium (Fig. 2H). Although cells in other regions of the embryo also express *fibronectin 1* (*fn1*) (Zhao et al., 2001), *cldna* expression marks the ear (Kollmar et al., 2001) and the posterior lateral line (not shown). In contrast to wild-type embryos, however, these residual otic cells form only a tight cluster, resembling an epithelial ball, and never produce a vesicle or other morphological features of the ear.

Knockdown of *dlx3b*, *dlx4b* and *sox9a* functions is sufficient to block formation of the ear

Our analysis of Df^{b380} mutants suggested that the functioning of some combination of the *dlx3b*, *dlx4b* and *sox9a* genes is required for specification of the otic placode. Based solely on this analysis, however, we could not rule out the possibility that other genes are also required, because the deficiency is rather large. To distinguish between these possibilities, we used morpholino antisense oligonucleotides (MOs) that block translation or splicing of mRNA from individual target genes when injected into zebrafish embryos (Nasevicius and Ekker, 2000; Draper et al., 2001).

Knockdown of all three transcription factors phenocopies the Df^{b380} deficiency mutant phenotype. When *dlx3b*-MO,

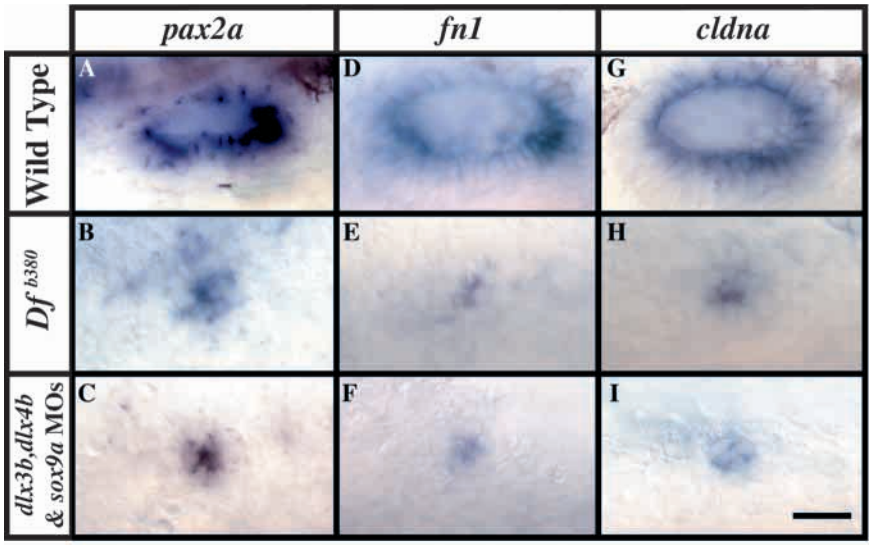

Fig. 2. Knockdown of Dlx3b, Dlx4b and Sox9a functions mimics the *Df*^{b380} mutant ear phenotype. (A,D,G) Otic vesicles of wild-type embryos express *pax2a*, *fn1* and *cldna*. (B,E,H) A few cells in *Df*^{b380} mutants form a small epithelial ball and express the same markers (83/196 *Df*^{b380} mutants expressed *pax2a*, 11/17 expressed *fn1* and 10/20 expressed *cldna*). (C,F,I) Injection of a mixture of *dlx3b*-MO, *dlx4b*-MO and *sox9a*-MO produces a similar, small ball of cells that express the same markers (24/56 expressed *pax2a*, 8/20 expressed *fn1* and 2/7 expressed *cldna*). Developmental stage: Prim-5 (24 h). Side views, anterior towards the left, dorsal towards the top. Scale bar: 25 μm.

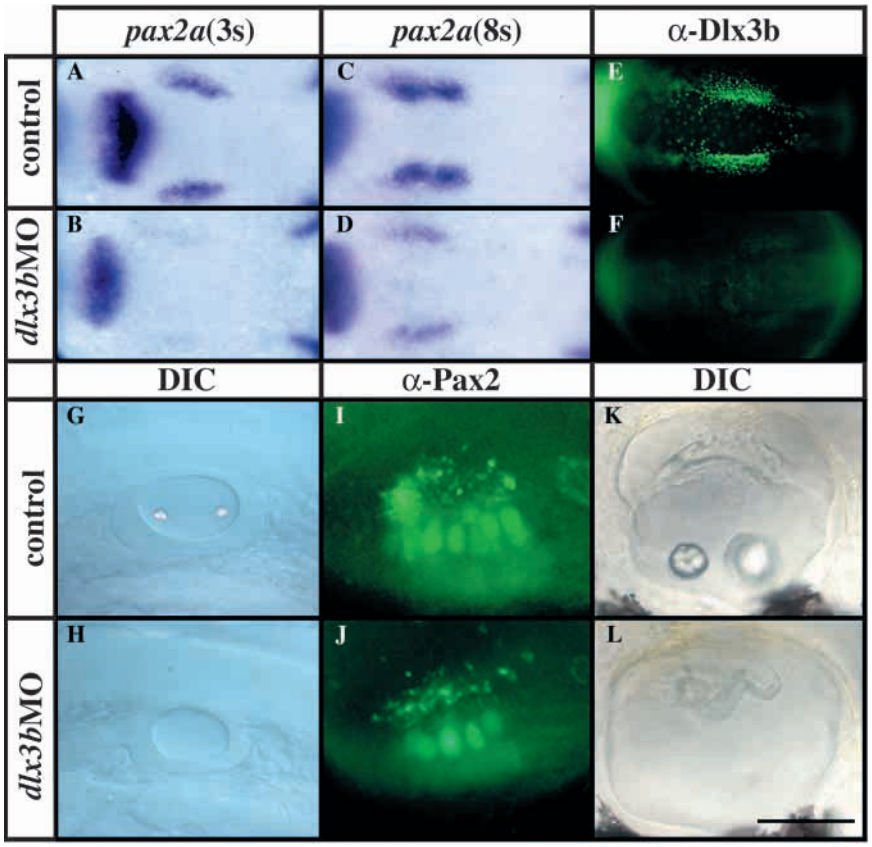

Fig. 3. Dlx3b function is required for generation of the full complement of otic sensory hair cells and semi-circular canals. (A,C,I) In normal (control) embryos, *pax2a* expression marks the presumptive otic placode at the three-somite (3s; A) and eight-somite (8s; C) stages. By high-pec stage (43h; I), otic sensory hair cells express Pax2a as indicated by antibody (α-Pax2; I) labeling. (B,D,J) In embryos injected with *dlx3b*-MO, *pax2a* expression is absent early (B; three-somite stage; 16/60 embryos) and reduced later (D; eight-somite stage; 5/17 embryos). By high-pec stage (J; 43 h) about half the normal number of Pax2-expressing otic sensory hair cells are apparent after knock down of *dlx3b* function by morpholino injection. Hair cell numbers as indicated by α-Pax2 labeling: wild-type 11.9±0.8 (*n*=34), *dlx3b*-MO 6.9±1.5 (*n*=49), *dlx4b*-MO 9.4±1.2 (*n*=7), *dlx3b* + *dlx4b* MOs 0.2±0.4 (*n*=18). (E,F) A Dlx3b antibody (α-Dlx3b) labels Dlx3b-expressing cells at the six-somite stage in normal embryos (E), but not after injection of *dlx3b*-MO (F). (G,H,K,L) Knock down of *dlx3b* function blocks formation of the otoliths (G,H; prim-5 stage, 24 h) and subsequent formation of the semi-circular canals (K,L; pec-fin stage). Twenty-eight percent of 356 injected embryos lacked both otoliths and semi-circular canals; all embryos injected with *dlx3b*-MO and *dlx4b*-MO lacked otoliths (data not shown). (A-F) Dorsal views, anterior towards the left; (G-L) side views, anterior towards the left, dorsal towards the top. Scale bar: 107 μm for A-D; 110 μm for E,F; 73 μm for G,H,K,L; 25 μm for I,J.

dlx4b-MO and *sox9a*-MO are injected in combination into wild-type embryos, formation of the otic placode fails and we observe only a few residual *pax2a*-expressing cells as in *Df*^{b380} mutants (Fig. 2C). These residual cells form a small epithelial ball and also express *fn1* and *cldna* (Fig. 2F,I), as do *Df*^{b380} mutants (Fig. 2E,H). These results demonstrate that the combined loss of Dlx3b, Dlx4b and Sox9a functions is sufficient to account for the *Df*^{b380} mutant otic phenotype. To study the requirements and individual roles of these three transcription factors in otic specification, we then injected MOs directed against single genes or combinations of two genes.

Dlx3b function is required for early and complete maturation of the otic placode and vesicle. Injection of *dlx3b*-MO morpholinos into wild-type embryos delays specification of the otic placode as indicated by delayed and reduced *pax2a* expression (Fig. 3A-D) and morphological maturation (Fig. 3G,H,K,L). The *dlx3b*-MO also affects later differentiation of the otic vesicle; the vesicle fails to achieve either its normal

size or numbers of otoliths (Fig. 3H,L) and sensory hair cells (Fig. 3I,J). Formation of epithelial protrusions and subsequent semicircular canals also fails (Fig. 3K,L). To ensure that the *dlx3b*-MO effectively knocks down *dlx3b* function, we raised a monoclonal antibody specific for Dlx3b protein and demonstrated absence of labeling after *dlx3b*-MO injection (Fig. 3E,F). These results are consistent with an absence of detectable levels of protein and provide additional support for the conclusion that Dlx3b is required for otic development. However, because the effects of *dlx3b*-MO on the ear are less severe than the Df^{b380} mutant phenotype, other genes missing in the Df^{b380} deficiency must also be required for otic placode specification.

Dlx4b has a less significant function than Dlx3b in otic development. Injection of *dlx4b*-MO has little effect on specification of the placode during early segmentation stages, as indicated by *pax2a* expression and by morphological observations (data not shown). By contrast, *dlx4b*-MO injection produced a very severe reduction in development of the medial fin fold (data not shown), another site of *dlx4b* expression (Ellies et al., 1997) suggesting that *dlx4b*-MO effectively blocks Dlx4b function. By prim-15 (30 h) stage, the otic vesicle is slightly smaller than normal after *dlx4b*-MO injection, but the normal number of otoliths and hair cells form. However, when the *dlx4b*-MO and *dlx3b*-MO are combined, an additive effect is seen; otoliths fail to form in the majority of embryos (Solomon and Fritz, 2002), the otic vesicle is smaller than after injection of either morpholino alone and essentially no sensory hair cells or epithelial protrusions form (data not shown). Nevertheless, the combined effect of both morpholinos is less severe than the Df^{b380} mutant phenotype.

Knockdown of Sox9a function by morpholino (*sox9a*-MO) injection has a relatively mild effect on otic specification, resulting in a slightly reduced vesicle with a normal number of otoliths (data not shown). To ensure that Sox9a function was blocked, we used morpholinos directed against splice donor and acceptor sites that would be expected to interfere with splicing of the *sox9a* pre-mRNA. Consistent with this interpretation, we found, using mRNA in situ hybridization, that *sox9a* message localizes in nuclei after *sox9a*-MO injection as we previously reported (Yan et al., 2002), suggesting that the morpholinos effectively block splicing. We obtained similar results with *sox9a* translation blocking and mRNA splice blocking MOs. The effect of *sox9a*-MO on otic development is more severe than the otic phenotype of *jef* (*sox9a*) mutants (data not shown), probably because of partial early function of this mutant allele (Yan et al., 2002).

Function of Dlx3b, Dlx4b and Sox9a transcription factors is sufficient to rescue otic placode specification in Df^{b380} mutants

If combined loss of the *dlx3b*, *dlx4b* and *sox9a* genes is responsible for the absence of otic placode specification in Df^{b380} mutants, then restoring wild-type function of only these genes should rescue the mutant phenotype. To test this prediction, we injected wild-type mRNAs for each gene into Df^{b380} mutant embryos. Although neither *dlx4b* nor *sox9a* mRNA rescues the mutant phenotype, *dlx3b* mRNA partially restores otic placode specification as indicated by *pax2a* expression and morphology (Fig. 4C,G). Injection of a combination of all three mRNAs into Df^{b380} mutants produces a much more robust rescue; the size of the placode, the number of *pax2a*-expressing cells and the level of *pax2a* expression are comparable with wild-type values (Fig. 4D,H). Rescue of later otic development is variable and less complete, probably because of degradation of the injected mRNAs, as we have previously shown for injected DNA (Westerfield et al., 1992).

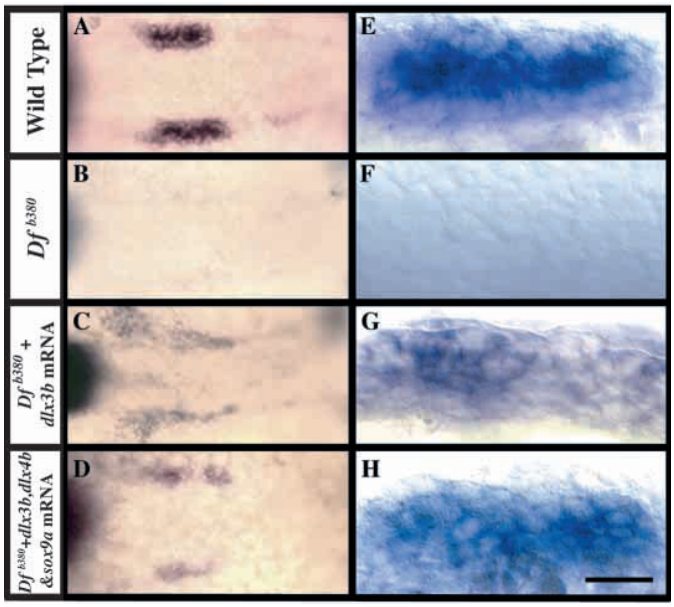

Fig. 4. Restoring Dlx3b, Dlx4b and Sox9a functions together rescues the Df^{b380} mutant ear phenotype at the 10-somite stage. (A,E) Wild-type embryos express *pax2a* in the presumptive otic placodes. (B,F) Df^{b380} mutant embryos lack early otic expression of *pax2a* (50/51 embryos). (C,G) Injection of wild-type *dlx3b* mRNA into Df^{b380} mutants partially restores otic *pax2a* expression (13/30 embryos). (D,H) Injection of wild-type *dlx3b*, *dlx4b* and *sox9a* mRNAs into Df^{b380} mutants restores otic *pax2a* expression to nearly normal levels (22/65 embryos). In other experiments, 8/30 Df^{b380} embryos injected with *dlx3b* and *dlx4b* and 11/33 injected with *dlx3b* and *sox9a* showed rescued *pax2a* expression. (A-D) Dorsal views, anterior towards the left; (E-H) side views, anterior towards the left, dorsal towards the top. Scale bar: 100 μm in A-D; 31 μm in E-H.

sox9b also participates in otic specification

Our observation that a few residual cells express otic markers in Df^{b380} mutants (Fig. 2) suggests the possibility that factors in addition to *dlx3b*, *dlx4b* and *sox9a* participate in otic specification. We have previously shown that the *sox9a* duplicate, *sox9b*, is also expressed in the otic placode and vesicle (Chiang et al., 2001). To examine its potential role in otic specification, we compromised its function using morpholino injection. Reduction of either *sox9a* function, in *jef* (*sox9a*) mutants (Fig. 5C), or *sox9b* function by morpholino injection (Fig. 5B) has little or no effect on formation of the otic vesicle. Compromising both genes results in a more severe reduction in otic specification, although, as in Df^{b380} mutants, some residual scattered cells still express otic markers (Fig. 5D). Knockdown of *sox9b* in Df^{b380} mutants completely blocks all signs of otic specification (Fig. 5F). Thus, like Sox9a, Sox9b participates in otic specification; Sox9b function in Df^{b380} mutants presumably accounts for the few residual otic cells that form in the absence of *dlx3b*, *dlx4b* and *sox9a*.

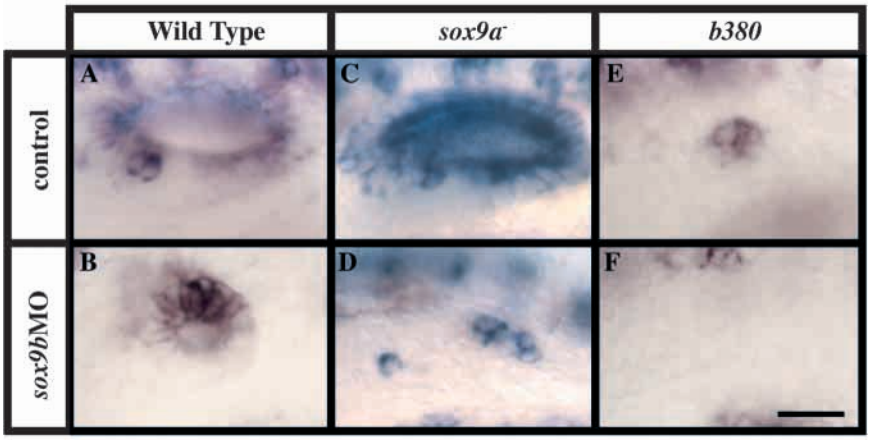

Fig. 5. *sox9b* functions in otic specification. (A,B) The splice-blocking morpholino against *sox9b* (*sox9b*MO) significantly reduces the size of the otic vesicle (B, *n*=40 embryos), compared with that of wild-type control embryos (A). (C,D) In *jellyfish* (*jef*) mutants that harbor a retroviral insertion in the *sox9a* gene (*jef*^{hil134}) (Amsterdam et al., 1999; Yan et al., 2002), injecting *sox9b*-MOs results in the loss of a morphologically recognizable otic vesicle (*n*=9 embryos), although a few dispersed *pax2a*-positive cells persist (D). In uninjected *jef* (*sox9a*) mutants (C, *n*=6 embryos), otic vesicles are slightly smaller than in wild-type control embryos (A). (E,F) Injecting *sox9b*-MO blocks formation of the residual otic cells of *Df*^{b380} (4/6 *Df*^{b380} embryos had residual *pax2a*-expressing cells, only 2/12 *Df*^{b380} embryos had residual otic cells after injection with *sox9b*-MO). (A,B,E,F) prim-12 (28 h); (D,F) prim 25 (36 h). Side views, anterior towards the left, dorsal towards the top. Scale bar: 25 μm.

sox9a but not *dlx3b, dlx4b* or *sox9b* expression requires Fgf3 and Fgf8 signaling

Recent studies have implicated combined, redundant functions of Fgf3 and Fgf8 in zebrafish otic placode induction (Philips et al., 2001; Léger and Brand, 2002; Maroon et al., 2002). To learn whether Fgf3 and Fgf8 function in a common pathway with Dlx3b, Dlx4b, Sox9a and/or Sox9b, we examined expression of *fgf3* and *fgf8* in *Df*^{b380} mutants and expression of the four transcription factors in *fgf8*$^{-}$ mutants (Reifers et al., 1998) and after injection of *fgf3* morpholinos (*fgf3*-MO) into wild-type embryos. Expression of *fgf3* and *fgf8* is relatively normal in *Df*^{b380} mutants; we observed no change in *fgf8* expression and only a slight increase in *fgf3* expression in rhombomere 4 (data not shown).

Reduction of Fgf8 function in *fgf8*$^{-}$ mutants significantly reduces *sox9a* otic expression (Fig. 6C), whereas knockdown of Fgf3 by *fgf3*-MO injection, results in a more modest reduction of *sox9a* otic expression (Fig. 6B). Injection of *fgf3*-MO into *fgf8*$^{-}$ mutants results in complete absence of *sox9a* expression in the region where the otic placode would normally form (Fig. 6D). Thus, Fgf3 and Fgf8 appear to act synergistically to support *sox9a* expression, just as they apparently act together to support otic development (Philips et al., 2001; Léger and Brand, 2002; Maroon et al., 2002). Reduction of Fgf signaling has a similar although somewhat less significant effect on *sox9b* expression (Fig. 6E-H). Residual *sox9b* expression in the otic area, even when both *fgf3* and *fgf8* are compromised, is consistent with Fgf-independent regulation of *sox9b*.

By contrast, *dlx3b* expression is relatively unaffected by reduction of Fgf signaling. Knockdown of Fgf3 function by injection of *fgf3*-MO, has no significant effect on the *dlx3* otic expression pattern (Fig. 6J). Loss of Fgf8 function in *fgf8*$^{-}$ mutants or *fgf3*-MO injection into *fgf8*$^{-}$ mutants results in only a slight narrowing of the *dlx3b* (Fig. 6K,L) and *dlx4b* (not shown) expression domains and significant numbers of Dlx3b-expressing cells remain, although they are scattered along the side of the hindbrain (Fig. 7D,F) rather than being well organized into an otic epithelium (Fig. 7C,E).

The reduction in size of the *dlx3b* expression domain when Fgf3 and Fgf8 signaling is blocked is probably due to the loss of Sox9a function. Consistent with this hypothesis, the *dlx3b*

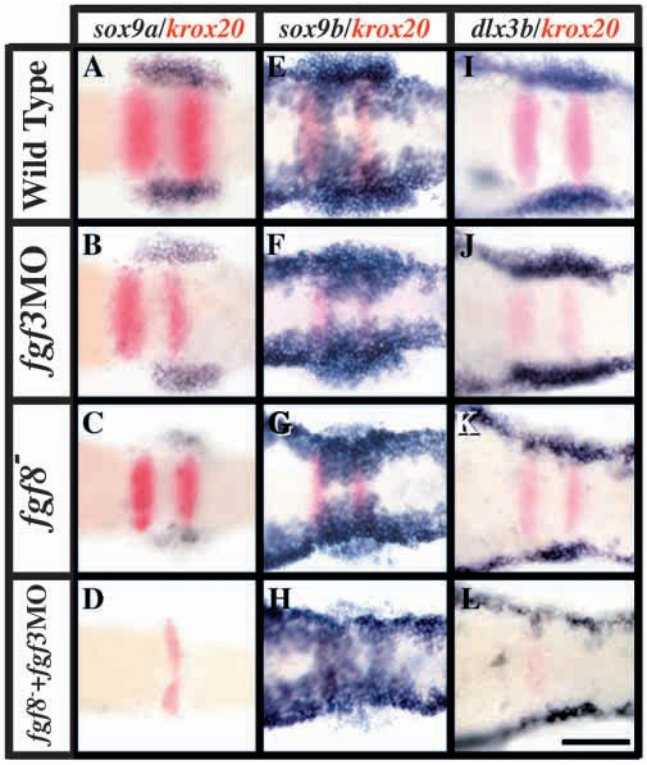

Fig. 6. Fgf3 and Fgf8 signaling together is required for otic expression of *sox9a* but not *sox9b* or *dlx3b*. (A-D) Cells of the presumptive otic placodes express *sox9a* in wild-type embryos (A), at somewhat reduced levels after *fgf3*-MO injection (B), at more reduced levels in *fgf8*$^{-}$ mutant embryos (C) and at undetectable levels in *fgf8*$^{-}$ embryos injected with *fgf3*-MO (D; *n*=8). (E-H) Cells of the presumptive otic area and cranial neural crest (Li et al., 2002) express *sox9b* in wild-type embryos (E) and *fgf3*-MO injected embryos (F). Expression of *sox9b* in the otic region is slightly reduced in *fgf8*$^{-}$ embryos (G) and more significantly reduced, although not completely eliminated, in *fgf8*$^{-}$ embryos injected with *fgf3*-MO (H; *n*=10). *sox9b* expression in cranial crest is apparently unaffected by reduced *fgf3* and *fgf8* expression. (I-L) Otic expression of *dlx3b* is much less affected by reduction of Fgf signaling (*n*=16). Similar results were obtained for *dlx4b* (not shown). Expression of *egr2* (*krox20*) in red indicates the locations of rhombomeres 3 and 5. Four-somite stage. Dorsal views, anterior towards the left. Scale bar: 110 μm.

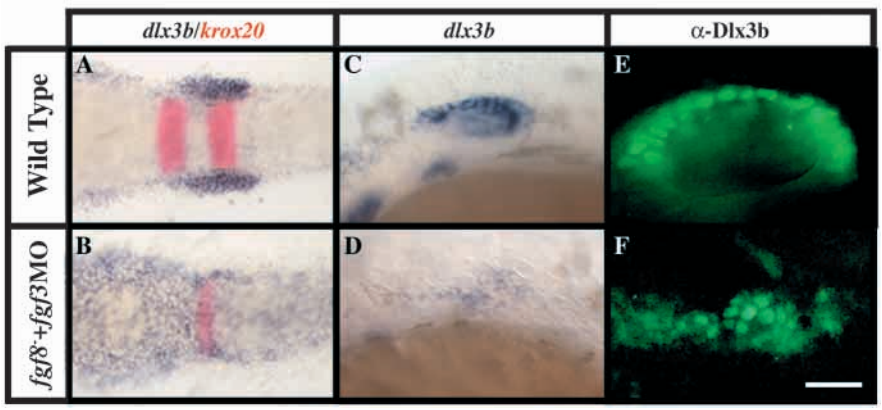

Fig. 7. Removal of both Fgf3 and Fgf8 signaling reduces the number, but does not eliminate Dlx3b-expressing otic cells. (A,B) Early expression of *dlx3b* in cells of the presumptive otic placode (A) is reduced in *fgf8*$^{-}$ mutants injected with *fgf3*-MO (B; *n*=18). (C-F) Later, at prim-6 stage (25h), *dlx3b*-expressing cells persist in *fgf8*$^{-}$ embryos injected with *fgf3*-MO (D) and the α-Dlx3b antibody shows that the residual Dlx3b-expressing cells are scattered (F), rather than being organized into an otic epithelium (E). Similar results were obtained in 3/15 injected mutants. (A,B) Dorsal view, anterior towards the left; (C-F) side view, anterior towards the left and dorsal towards the top. Scale bar: 100 μm for A-D; 25 μm for E,F.

and *sox9a* expression domains largely overlap in the otic region (Fig. 8A,B) and we found that knockdown of *sox9a* by itself results in a reduction in the *dlx3b* expression domain (Fig. 8C,D) similar to loss of Fgf3 and Fgf8 function (Fig. 6L). Reciprocally, knockdown of *dlx3b* produces a reduction in the *sox9a* expression domain (Fig. 8E,F). By contrast, knockdown of *sox9b* reduces *sox9a* expression slightly (Fig. 8G,H) but has little effect on *dlx3b* or *dlx4b* expression (not shown). Knockdown of *dlx4b* had only a slight effect on *sox9a* or *sox9b* expression (not shown), but *dlx3b*-MO combined with *dlx4b*-MO had a greater effect than either alone (Fig. 8I,J and data not shown). Together, these results suggest that the function of Fgf3 and Fgf8 in otic induction is independent of Dlx3b and Dlx4b, but is mediated at least partly by Sox9a and Sox9b. Moreover, we found that the *dlx3b-dlx4b* and *sox9a* genes reciprocally regulate each other's expression.

Residual otic cells that form in *Df*^{b380} mutants require Fgf signaling

Our observation that some aspects of Fgf3 and Fgf8 function in otic specification are independent of Dlx3b and Dlx4b raised the possibility that the residual otic cells that form in *Df*^{b380} mutants require Fgf3 and Fgf8 function. We tested this possibility by examining otic specification in *Df*^{b380} mutants with compromised Fgf signaling. Although a few otic cells form in *Df*^{b380} mutants injected with *fgf3* MO (Fig. 9C), we observed no signs of otic cells morphologically or by *pax2a* expression in *Df*^{b380};*fgf8*$^{-}$ double mutants (Fig. 9D). These results support the interpretation that in the absence of *dlx3b*, *dlx4b* and *sox9a*, Fgf signaling is still capable of inducing a few cells to express characteristics of otic cells, although these cells fail to form a functional ear. These are presumably Fgf-dependent *sox9b*-expressing cells (Fig. 6E-H), because all signs of otic specification are also missing when we knockdown *sox9b* expression in *Df*^{b380} mutants (Fig. 5F). The few otic cells that develop in *Df*^{b380} mutants or when either Fgf3 or Fgf8 signaling is compromised, form a small epithelial ball that resembles the early stages of otic vesicle formation (Fig. 9B,C,F,G). Further development fails. Knockdown of both Fgf signals, when *dlx3b*, *dlx4b* and *sox9a* are still intact,

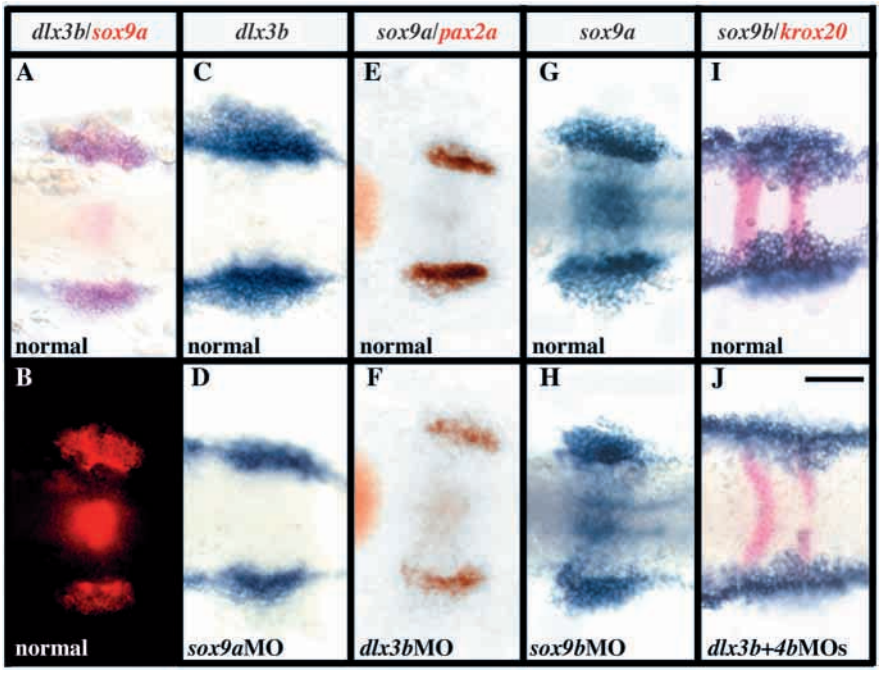

Fig. 8. Dlx3b and Sox9a crossregulate each other's expression in the otic placode. (A,B) *dlx3b* (blue) and *sox9a* (red) colocalize in the presumptive otic placode at the four-somite stage as shown with brightfield (A) and fluorescence (B) optics. *sox9a* is also expressed in presumptive rhombomere 4. (C,D) *dlx3b* expression is reduced in the otic placode after injection of *sox9a*-MO (30/37 embryos). (E,F) *sox9a* expression (blue) is reduced in the otic placode after injection of *dlx3b*-MO (44/50 embryos). *pax2a* expression is shown in red. (G,H) *sox9b*-MO produces a very slight reduction in *sox9a* expression in the otic region (15/18 embryos). (I,J) *sox9b* expression is significantly reduced by *dlx3b*-MO plus *dlx4b*-MO injection (16/18 embryos). We observe a similar reduction in *sox9b* expression in *Df*^{b380} mutants (not shown). Expression of *egr2* (*krox20*) in red indicates the locations of rhombomeres 5 and 6. Four-somite stage (11 h). Dorsal views, anterior towards the left. Scale bar: 100 μm in A-F.

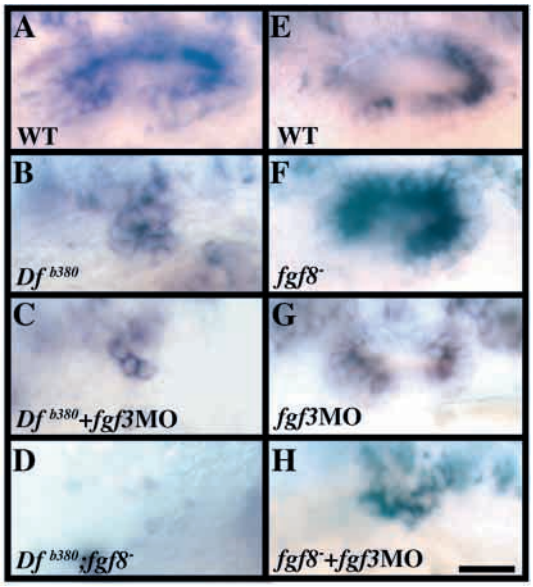

Fig. 9. The residual otic cells that form in Df^{b380} mutants require Fgf3 and Fgf8 signaling. (A,B) Loss of *dlx3b*, *dlx4b* and *sox9a* function in Df^{b380} mutants results in formation of only a few residual otic cells, as indicated by *pax2a* expression, that form a small epithelial ball (19/44 Df^{b380} embryos). (C) Injection of *fgf3*-MO into Df^{b380} mutants further reduces the number of otic cells, but the residual cells still form an epithelial-like structure (9/21 embryos). (D) Df^{b380};$fgf8^{-}$ double mutants lack all detectable otic cells (11/11 embryos). (E,F) $fgf8^{-}$ mutants form a somewhat variably smaller but otherwise fairly normal otic vesicle. (G) Injection of *fgf3*-MO into wild-type embryos results in a small and somewhat disorganized otic vesicle. (H) Injection of *fgf3*-MO into $fgf8^{-}$ mutants results in a very reduced number of disorganized otic cells (25/26 embryos). More than half of the injected embryos form a relatively large placode or vesicle-like otic mass (not shown), suggesting a less severe otic phenotype compared with $fgf8^{-}$ mutants injected with *fgf3*-MO. Prim-5 (24h). Side views, anterior towards the left, dorsal towards the top. Scale bar: 25 μm.

results in development of a similar number of cells that express otic markers such as *pax2a*, but in contrast to Dlx3b, Dlx4b and Sox9a depletion, these putative otic cells are scattered along the side of the hindbrain and fail to assemble into an epithelial structure (Fig. 7D,F; Fig. 9H).

DISCUSSION

Previous studies have implicated the signaling molecules Fgf3 and Fgf8 (Vendrell et al., 2000; Phillips et al., 2001; Léger and Brand, 2002), and the transcription factors Dlx3b and Dlx4b (Ekker et al., 1992; Akimenko et al., 1994; Ellies et al., 1997; Solomon and Fritz, 2002) in induction and specification of the vertebrate inner ear. To help define how these various factors interact and their specific roles in otic induction, we analyzed zebrafish $fgf8^{-}$ mutants, Df^{b380} deficiency mutants that lack *dlx3b*, *dlx4b* and *sox9a*, and embryos injected with morpholinos to knockdown the functions of these genes. To analyze Fgf3 and Sox9b functions, we used *fgf3*-MO and *sox9b*-MO, respectively,

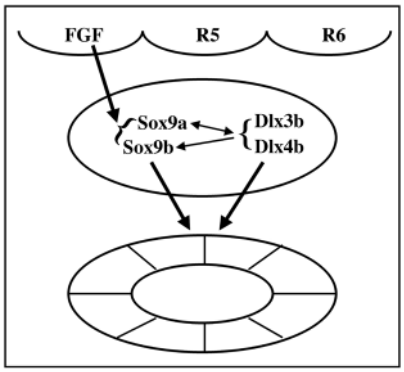

Fig. 10. Fgf3- and Fgf8-dependent and -independent pathways for otic development. Model to summarize potential interactions between hindbrain Fgf signals and otic placode transcription factors. (Top) Fgf3 and Fgf8 (FGF) are expressed at high levels by hindbrain rhombomere 4 (Maves et al., 2002; Walshe et al., 2002). Adjacent rhombomeres are labeled R5 and R6. (Middle) Cells of the presumptive otic placode express *sox9b* and the three transcription factors deleted by the Df^{b380} mutation: *dlx3b*, *dlx4b* and *sox9a* (Fig. 1). Both *sox9a* (Fig. 6A-D) and to some extent *sox9b* (Fig. 6E-H) require Fgf signaling, whereas *dlx3b* (Fig. 6I-L) and *dlx4b* do not. *dlx3b* and *sox9a* crossregulate each other's expression in the placode (Fig. 8C-F) and *dlx3b* and *dlx4b* regulate *sox9b* (Fig. 8I,J). Thus, interactions between the Fgf3- and Fgf8-dependent factor, *sox9a*, and the relatively Fgf3- and Fgf8-independent factors (*sox9b*, *dlx3b* and *dlx4b*) are required for formation of the epithelium of the otic vesicle (bottom) and subsequent differentiation of the inner ear.

because mutations in the *fgf3* and *sox9b* genes have not yet been identified in zebrafish.

Fgf3- and Fgf8-dependent and -independent pathways of otic development

Our results provide evidence for Fgf3- and Fgf8-dependent and -independent pathways in otic development (Fig. 10). We found that loss of either Fgf3 and Fgf8 function or functions of Dlx3b, Dlx4b and Sox9a transcription factors missing in the Df^{b380} deficiency mutation results in nearly complete loss of otic tissue, although a few residual cells express otic markers. Loss of both Fgf3 and Fgf8 function, and functions of the three transcription factors completely blocks all indications of otic induction. The Fgf-dependent and -independent pathways appear to act synergistically. The number of otic cells is drastically reduced in Dlx3b-and Dlx4b-deficient or Fgf3- and Fgf8-deficient embryos. Providing either Dlx3b and Dlx4b or Fgf3 and Fgf8 function produces only limited otic specification, much less than when both pathways are active.

Previous studies, using three markers, *pax8*, *pax2a* and *dlx3b*, to examine the Fgf dependence of initial induction of the otic placode, produced somewhat differing results (Phillips et al., 2001; Léger and Brand, 2002; Maroon et al., 2002). Using morpholinos to knockdown Fgf3 and Fgf8, Léger and Brand (Léger and Brand, 2002) reported loss or strong reduction of *pax2a* and *pax8* expression in the otic region; Maroon et al. (Maroon et al., 2002) found less severe defects. By injecting *fgf3*-MO into $fgf8^{-}$ mutants, Léger and Brand and Phillips et al. found strong reduction of *pax2a* and *pax8* (Léger and Brand, 2002; Phillips et al., 2001) Using SU5402, a general inhibitor of Fgf receptors, Léger and Brand (Léger

and Brand, 2002) reported complete loss of *pax2a* and *pax8*; Maroon et al. (Maroon et al., 2002) obtained similar results for *pax2a* but found that *pax8* was unaffected unless the inhibitor was applied at later stages. Using SU5402, Léger and Brand (Léger and Brand, 2002) found that initial *dlx3b* expression is independent of Fgf signaling, but later expression in the otic region is reduced. They reported similar results with *fgf3*-MO + *fgf8*-MO. Although Maroon et al. did not examine the earliest stages of *dlx3b* expression, they found that *dlx3b* expression at later stages was lost in some experiments but only reduced in others after Fgf-MO injections. Phillips et al. did not examine *dlx3b* expression (Phillips et al., 2001). Although the results of these studies differ somewhat, possibly because of differences in experimental conditions, all three groups similarly conclude that Fgf3 and Fgf8 are required for initial otic induction. Our results show that although most signs of otic induction are missing when Fgf3 and Fgf8 signaling is blocked, a few residual otic cells form as indicated by expression of *pax2a*, *dlx3b*, *fn1* and *cldna*. The previous studies may well have missed these remaining otic cells we have identified, probably because they are few in number and typically scattered along the side of the hindbrain, rather than being organized into an easily recognizable vesicle. Our results also provide an explanation for apparent discrepancies among the previous studies of the Fgf dependence of *dlx3b* expression. We show that *sox9a* expression requires *fgf3* and *fgf8*; *sox9a*, in turn, is required for normal expression of *dlx3b* and *dlx4b*. Thus, induction and early patterning of *dlx3b* and *dlx4b* expression are unaffected by blocking Fgf3 and Fgf8 signaling, but their later expression in the otic region is reduced because of loss of *sox9a*.

Consistent with previous studies that suggested Fgf3 and Fgf8 have redundant functions in hindbrain (Maves et al., 2002; Walshe et al., 2002) and otic development (Philips et al., 2001; Léger and Brand, 2002; Maroon et al., 2002), we found that reduction of either Fgf3 or Fgf8 signaling produces a partial loss of *sox9a* and *sox9b* expression (Fig. 6B,C,F,G) and a smaller or somewhat disorganized otic vesicle (Fig. 9F,G). Reduction of both Fgfs (Fig. 6D,H; Fig. 9H) produces a greater defect than reduction of either alone. However, recent studies suggest that Fgf3 and Fgf8 have different downstream targets (Reifers et al., 2000). Loss of Fgf8 function (in *fgf8*$^{-}$ mutants) consistently produces a more severe phenotype than knockdown of Fgf3 function alone by injection of *fgf3* MO, suggesting that although Fgf3 and Fgf8 may have overlapping functions, Fgf8 apparently plays a more significant role in otic induction than Fgf3, perhaps because of its earlier and more widespread expression (Reifers et al., 1998; Maves et al., 2002).

Genetic interactions of *sox9a* and *sox9b* with *fgf3*, *fgf8*, *dlx3b* and *dlx4b*

Part of Fgf3 and Fgf8 function in otic development is mediated by Sox9a and Sox9b. We found that in the otic region after Fgf3 and Fgf8 reduction, *sox9a* expression is lost (Fig. 6D) and *sox9b* expression is reduced although not completely eliminated (Fig. 6H). The *dlx3b* and *dlx4b* expression domain is reduced by knockdown of *sox9a* expression, and there is a similar reduction in *sox9a* expression by knockdown of *dlx3b* and *dlx4b* (Fig. 8C-F). Depletion of Fgf3 and Fgf8 signaling similarly reduces *dlx3b* and *dlx4b* expression (Fig. 6H), presumably because of loss of *sox9a* function. By contrast, reduction of *sox9b* expression has little effect on *dlx3b* and *dlx4b* expression, although *sox9b* expression depends on Dlx3b and Dlx4b (Fig. 8I,J). These results indicate that *sox9a* interacts genetically with both the Fgf3- and Fgf8-dependent and -independent pathways. Thus, *sox9a* apparently plays a central role in coordinating otic development.

Previous studies have shown that *pax8* expression is also reduced or lost in *fgf8*$^{-}$ mutants injected with *fgf3*-MO (Philips et al., 2001; Léger and Brand, 2002) (but see Maroon et al., 2002). In addition, *pax8* expression persists in the absence of the *dlx3b*, *dlx4b* and *sox9a* genes (Solomon and Fritz, 2002) (D.L., H.C. and M.W., unpublished). Thus, Fgf3 and Fgf8 signaling appears to act through at least two genetically distinct pathways in the otic placode: one dependent upon Sox9a and the other mediated by something else, possibly Pax8 or other, as yet unidentified factors. Although *pax8* expression is unaffected by reduction of *sox9a*, we have not yet determined whether Pax8 acts in the same or different pathways with Sox9a and Sox9b.

Fgf3 and Fgf8 functions in otic induction and morphogenesis

Our results may provide insight into how Fgf3 and Fgf8 growth factors function in otic development. Previous studies have indicated that FGF3 directs morphogenesis of the avian otic vesicle (Vendrell et al., 2000). We found that the residual otic cells in Fgf3- and Fgf8-deficient embryos failed to form an epithelial structure (Fig. 7D,F; Fig. 9H), whereas the residual otic cells in *Df*^{b380} mutants, with Fgf3 and Fgf8 signaling still intact, form small epithelial balls (Fig. 2B,E,H; Fig. 9B). This might indicate that Fgf3-Fgf8 signaling that is normally localized to rhombomere 4 ‘organizes’ the placode cells into an epithelium that subsequently forms the otic vesicle. We have recently provided evidence for a similar Fgf3- and Fgf8-dependent activity of rhombomere 4 in organizing posterior hindbrain segments (Maves et al., 2002). Our previous fate map analysis of the nose demonstrated that cells from a relatively large area at the lateral edge of the neural plate converge to form the olfactory placode and subsequent epithelium (Whitlock and Westerfield, 2000). A similar mechanism may occur during otic placode development. Perhaps in the absence of Fgf3 and Fgf8 signals from rhombomere 4, cells fail to converge properly to this organizing region and, hence, cannot form the otic epithelium.

We thank Kate Barald, Bon-chu Chung, Bruce Draper, Andreas Fritz, Kiyoshi Kikuchi and Charles Kimmel for helpful discussions. Jocelyn McAuley, Anni O’Shea, Jeremy Wegner and Amelia Westerfield provided technical support. Supported by NIH (R01 DC04186, P01 HD22486 and NS17963) and the Canadian Institutes of Health Research.

REFERENCES

Akimenko, M.-A., Ekker, M., Wegner, J., Lin, W. and Westerfield, M. (1994). Combinatorial expression of three zebrafish genes related to *Distal-less*: part of a homeobox gene code for the head. *J. Neurosci.* **14**, 3475-3486.

Amsterdam, A., Burgess, S., Golling, G., Chen, W., Sun, Z., Townsend, K., Farrington, S., Haldi, M. and Hopkins, N. (1999). A large-scale insertional mutagenesis screen in zebrafish. *Genes Dev.* **13**, 2713-2724.

Baker, C. V. H. and Bronner-Fraser, M. (2001). Vertebrate cranial placodes. I. Embryonic induction. *Dev. Biol.* **232**, 1-61.

Bi, W., Huang, W., Whitworth, D. J., Deng, J. M., Zhang, Z., Behringer, R. R. and de Crombrugghe, B. (2001). Haploinsufficiency of Sox9 results in defective cartilage primordia and premature skeletal mineralization. *Proc. Natl. Acad. Sci. USA* **98**, 6698-6703.

Brand, M., Heisenberg, C. P., Warga, R. M., Pelegri, F., Karlstrom, R. O., Beuchle, D., Picker, A., Jiang, Y. J., Furutani-Seiki, M., van Eeden, F. J. M. et al. (1996). Mutations affecting development of the midline and general body shape during zebrafish embryogenesis. *Development* **123**, 129-142.

Cameron, F. J., Hageman, R. M., Cooke-Yarborough, C., Kwok, C., Goodwin, L. L., Sillence, D. O. and Sinclair, A. H. (1996). A novel germ line mutation in SOX9 causes familial campomelic dysplasia and sex reversal. *Hum. Mol. Genet.* **5**, 1625-1630.

Chiang, E., Pai, C.-I., Wyatt, M., Yan, Y.-L., Postlethwait, J. and Chung, B.-C. (2001). Two *sox9* genes on duplicated zebrafish chromosomes: expression of similar transcription activators in distinct sites. *Dev. Biol.* **231**, 149-163.

Couly, G. F., Coltey, P. M. and le Douarin, N. M. (1993). The triple origin of skull in higher vertebrates: a study in quail-chick chimeras. *Development* **117**, 409-429.

Dominguez, I., Itoh, K. and Sokol, S. Y. (1995). Role of glycogen synthase kinase 3ß as a negative regulator of dorsoventral axis formation in Xenopus embryos. *Proc. Natl. Acad. Sci. USA* **92**, 8498-8502.

Draper, B. W., Morcos, P. A. and Kimmel, C. B. (2001). Inhibition of zebrafish fgf8 pre-mRNA splicing with morpholino oligos: a quantifiable method for gene knockdown. *Genesis* **30**, 154-156.

Ekker, M. E., Akimenko, M.-A., BreMiller, R. and Westerfield, M. (1992). Regional expression of three homeobox transcripts in the inner ear of zebrafish embryos. *Neuron* **9**, 27-35.

Ellies, D., Stock, D., Hatch, G., Giroux, G., Weiss, K. and Ekker, M. (1997). Relationship between the genomic organization and the overlapping embryonic expression patterns of the zebrafish *dlx* genes. *Genomics* **45**, 580-590.

Foster, J. W., Dominguez-Steglich, M. A., Guioli, S., Kowk, G., Weller, P. A., Stevanoviâc, M., Weissenbach, J., Mansour, S., Young, I. D., Goodfellow, P. N. et al. (1994). Campomelic dysplasia and autosomal sex reversal caused by mutations in an SRY-related gene. *Nature* **372**, 525-530.

Fritz, A., Rozowski, M., Walker, C. and Westerfield, M. (1996). Identification of selected gamma-ray induced deficiencies in zebrafish using multiplex polymerase chain reaction. *Genetics* **144**, 1735-1745.

Fritzsch, B. F., Barald, K. F. and Lomax, M. I. (1997). Early embryology of the vertebrate ear. In *Development of the Auditory System* (ed. E. W. Rubel, A. N. Popper and R. R. Fay), pp. 80-145. New York, NY: Springer-Verlag.

Harrison, R. G. (1945). Relations of symmetry in the developing embryo. *Trans. Connecticut Acad. Arts Sci.* **36**, 277-330.

Hageman, R. M., Cameron, F. J. and Sinclair, A. H. (1998). Mutation analysis of the SOX9 gene in a patient with campomelic dysplasia. *Hum. Mutat. Suppl.* S112-S113.

Houston, C. S., Opitz, J. M., Spranger, J. W., Macpherson, R. I., Reed, M. H., Gilbert, E. F., Herrmann, J. and Schinzel, A. (1983). The campomelic syndrome: review, report of 17 cases, and follow-up on the currently 17-year-old boy first reported by Maroteaux et al., in 1971. *Am. J. Med. Genet.* **15**, 3-28.

Huang, W., Chung, U. I., Kronenberg, H. M. and de Crombrugghe, B. (2001). The chondrogenic transcription factor Sox9 is a target of signaling by the parathyroid hormone-related peptide in the growth plate of endochondral bones. *Proc. Natl. Acad. Sci. USA* **98**, 160-165.

Hukriede, N. A., Joly, L., Tsang, M., Miles, J., Tellis, P., Epstein, J. A., Barbazuk, W. B., Li, F. N., Paw, B., Postlethwait, J. H. et al. (1999). Radiation hybrid mapping of the zebrafish genome. *Proc. Natl. Acad. Sci. USA* **96**, 9745-9750.

Hutson, M. R., Lewis, J. E., Nguyen-Luu, D., Lindberg, K. H. and Barald, K. F. (1999). Expression of Pax2 and patterning of the chick inner ear. *J. Neurocytol.* **28**, 795-807.

Jacobson, A. G. (1963). The determination and positioning of the nose, lens and ear. II. The role of the endoderm. *J. Exp. Zool.* **154**, 285-291.

Jowett, T. and Yan, Y. L. (1996). Double fluorescent in situ hybridization to zebrafish embryos. *Trends Genet.* **12**, 387-389.

Kanzler, B., Kuschert, S. J., Liu, Y. H. and Mallo, M. (1998). Hoxa-2 restricts the chondrogenic domain and inhibits bone formation during development of the branchial area. *Development* **125**, 2587-2597.

Kimmel, C. B., Ballard, W. W., Kimmel, S. R., Ullmann, B. and Schilling, T. F. (1995). Stages of embryonic development of the zebrafish. *Dev. Dyn.* **203**, 253-310.

Kollmar, R., Nakamura, S. K., Kappler, J. A. and Hudspeth, A. J. (2001). Expression and phylogeny of claudins in vertebrate primordia. *Proc. Natl. Acad. Sci. USA* **98**, 10196-10201.

Krauss, S., Johansen, T., Korzh, V. and Fjose, A. (1991). Expression of the zebrafish paired box gene *pax* [*zf-b*] during early neurogenesis. *Development* **113**, 1193-1206.

Léger, S. and Brand, M. (2002). Fgf8 and Fgf3 are required for zebrafish ear placode induction, maintenance and inner ear patterning. *Mech. Dev.* **119**, 91-108.

Li, M., Zhao, C., Wang, Y., Zhao, Z. and Meng, A. (2002). Zebrafish *sox9b* is an early neural crest marker. *Dev. Genes Evol.* **212**, 203-206.

Lombardo, A. and Slack, J. M. (1998). Postgastrulation effects of fibroblast growth factor on *Xenopus* development. *Dev. Dyn.* **212**, 75-85.

Maroon, H., Walshe, J., Mahmood, R., Kiefer, P., Dickson, C. and Mason, I. (2002). Fgf3 and Fgf8 are required together for formation of the otic placode and vesicle. *Development* **129**, 2099-2108.

Maves, L., Jackman, W. and Kimmel, C. B. (2002). FGF3 and FGF8 mediate a rhombomere 4 signaling activity in the zebrafish hindbrain. *Development* **129**, 3825-3837.

Mendonsa, E. S. and Riley, B. B. (1999). Genetic analysis of tissue interactions required for otic placode induction in the zebrafish. *Dev. Biol.* **206**, 100-112.

Morasso, M. I., Grinberg, A., Robinson, G., Sargent, T. D. and Mahon, K. A. (1999). Placental failure in mice lacking the homeobox gene Dlx3. *Proc. Natl. Acad. Sci. USA* **96**, 162-167.

Nasevicius, A. and Ekker, S. C. (2000). Effective targeted gene 'knockdown' in zebrafish. *Nat. Genet.* **26**, 216-220.

Nakamura, S., Stock, D., Wydner, K. L., Bollekens, J. A., Takeshita, K., Nagai, B. M., Chiba, S., Kitamura, T., Freeland, T. M., Zhao, Z. et al. (1996). Genomic analysis of a new mammalian distal-less gene: *Dlx7*. *Genomics* **38**, 314-324.

Noden, D. M. and van de Water, T. R. (1986). The developing ear: tissue orgins and interactions. In *The Biology of Change in Otolaryngology* (ed. R. J. Ruben, T. R. van de Water and E. W. Rubel), pp. 15-46. Amsterdam: Elsevier.

Oxtoby, E. and Jowett, T. (1993). Cloning of the zebrafish krox-20 gene (krx-20) and its expression during hindbrain development. *Nucleic Acids Res.* **21**, 1087-1095.

Price, J. A., Wright, J. T., Kula, K., Bowden, D. W. and Hart, T. C. (1998). A common DLX3 gene mutation is responsible for tricho-dento-osseous syndrome in Virginia and North Carolina families. *J. Med. Genet.* **35**, 825-828.

Phillips, B. T., Bolding, K. and Riley, B. B. (2001). Zebrafish *fgf3* and *fgf8* encode redundant functions required for otic placode induction. *Dev. Biol.* **235**, 351-365.

Püschel, A. W., Westerfield, M. and Dressler, G. R. (1992). Comparative analysis of Pax-2 protein distributions during neurulation in mice and zebrafish. *Mech. Dev.* **38**, 197-208.

Reifers, F., Bohli, H., Walsh, E.C., Crossley, P. H., Stainier, D. Y. and Brand, M. (1998). Fgf8 is mutated in zebrafish *acerebellar* (*ace*) mutants and is required for maintenance of midbrain-hindbrain boundary development and somitogenesis. *Development* **125**, 2381-2395.

Repressa, J., Leon, Y., Miner, C. and Giraldez, F. (1991). The *int-2* proto-oncogene is reponsible for induction of the inner ear. *Nature* **353**, 561-563.

Robinson, G. W. and Mahon, K. A. (1994). Differential and overlapping expression domains of *Dlx-2* and *Dlx-3* suggest distinct roles for Distal-less homeobox genes in craniofacial development. *Mech. Dev.* **48**, 199-215.

Shapiro, S. D., Quattromani, F. L., Jorgenson, R. J. and Young, R. S. (1983). Tricho-dento-osseous syndrome: heterogeneity or clinical variability. *Am. J. Med. Genet.* **16**, 225-236.

Solomon, K. S. and Fritz, A. (2002). Concerted action of two *dlx* paralogs in sensory placode formation. *Development* **129**, 3127-3136.

Stock, D. W., Ellies, D. L., Zhao, Z. Y., Ekker, M., Ruddle, F. H. and Weiss, K. M. (1996). The evolution of the vertebrate *Dlx* gene family. *Proc. Natl. Acad. Sci. USA* **93**, 10858-10863.

Stone, L. S. (1931). Induction of the ear by the medulla and its relations to experiments on the lateralis system in amphibia. *Science* **74**, 577.

Thisse, C., Thisse, B., Schilling, T. and Postlethwait, J. H. (1993). Structure of the zebrafish *snail* gene and its expression in wild-type, *spadetail* and *no tail* mutant embryos. *Development* **119**, 1203-1215.

Torres, M. and Giráldez, F. (1998). The development of the vertebrate inner ear. *Mech. Dev.* **71**, 5-21.

Vendrell, V., Carnicero, E., Giráldez, F., Alonso, M. T. and Schimmang, T. (2000). Induction of inner ear fate by FGF3. *Development* **127**, 2011-2019.

Vidal, V. P. I., Chaboissier, M. C., de Rooij, D. G. and Schedl, A. (2001). *Sox9* induces testis development in XX transgenic mice. *Nat. Genet.* **28**, 216-217.

Waddington, C. H. (1937). The determination of the auditory placode in the chick. *J. Exp. Biol.* **14**, 232-239.

Wagner, M. H., Huth, J. R., Gronenborn, A. M. and Clore, G. M. (1995). Molecular basis of human 46X,Y sex reversal revealed from the three-dimensional solution structure of the human SRY-DNA complex. *Cell* **81**, 705-714.

Walshe, J., Maroon, H., McGonnell, I. M., Dickson, C. and Mason, I. (2002). Establishment of hindbrain segmental identity requires signaling by FGF3 and FGF8. *Curr. Biol.* **12**, 1117-1123.

Westerfield, M. (2000). *The Zebrafish Book: A Guide for the Laboratory Use of Zebrafish (*Danio rerio*)*. Eugene, OR: University of Oregon Press.

Westerfield, M., Wegner, J., Jegalian, B. G., de Robertis, E. M. and Püschel, A. W. (1992). Specific activation of mammalian Hox promotors in mosaic transgenic zebrafish. *Genes Dev.* **6**, 591-598.

Whitfield, T. T., Riley, B. B., Chiang, M.-Y. and Phillips, B. (2002). Development of the zebrafish inner ear. *Dev. Dyn.* **223**, 427-458.

Whitlock, K. E. and Westerfield, M. (2000). The olfactory placodes of the zebrafish form by convergence of cellular fields at the edge of the neural plate. *Development* **127**, 3645-3653.

Woo, K. and Fraser, S. (1998). Specification of the hindbrain fate in the zebrafish. *Dev. Biol.* **197**, 283-296.

Yan, Y.-L., Miller, C., Nissen, R., Singer, A., Liu, D., Kirt, A., Draper, B. W., Willoughby, J., Marcos, P. A., Chung, B.-C. et al. (2002). A zebrafish sox9 gene required for cartilage morphogenesis. *Development* **129**, 5065-5079.

Zhao, Q., Liu, X. and Collodi, P. (2001). Identification and characterization of a novel fibronectin in zebrafish. *Exp. Cell Res.* **268**, 211-219.